



Alcohol Fuel Cells at Optimal Temperatures

Tetsuya Uda,^a Dane A. Boysen,^b Calum R. I. Chisholm,^b and Sossina M. Haile^z

Department of Materials Science, California Institute of Technology, Pasadena, California 91125, USA

High-power-density alcohol fuel cells can relieve many of the daunting challenges facing a hydrogen energy economy. Here, such fuel cells are achieved using CsH_2PO_4 as the electrolyte and integrating into the anode chamber a Cu-ZnO/ Al_2O_3 methanol steam-reforming catalyst. The temperature of operation, $\sim 250^\circ\text{C}$, is matched both to the optimal value for fuel cell power output and for reforming. Peak power densities using methanol and ethanol were 226 and 100 mW/cm^2 , respectively. The high power output (305 mW/cm^2) obtained from reformat fuel containing 1% CO demonstrates the potential of this approach with optimized reforming catalysts and also the tolerance to CO poisoning at these elevated temperatures.
© 2006 The Electrochemical Society. [DOI: 10.1149/1.2188069] All rights reserved.

Manuscript received December 7, 2005. Available electronically March 31, 2006.

In recent years, significant attention has been directed to hydrogen gas as a fuel. However, major barriers remain to the implementation of a hydrogen-based energy economy, not the least of which is the absence of viable hydrogen storage and delivery technologies. Alcohols have stored energy densities several times that of standard compressed hydrogen (e.g., 1 L of methanol and ethanol are energetically equivalent to 4.4 and 5.8 L, respectively, of hydrogen gas compressed at 350 atm) and thus may address many of the challenges facing hydrogen as a fuel. Like hydrogen, alcohol fuels have the potential for being produced from renewable resources and thereby mitigating the production of carbon dioxide, a major greenhouse gas.¹ Yet, unlike hydrogen, they enjoy a well-developed fuel delivery infrastructure (second only to gasoline).

Implementation of alcohol fuels in fuel cells, energy conversion devices that combine the benefits of zero (regulated) emissions and high efficiency, requires that the fuel cell electrolyte be impermeable to the fuel. In addition, moderate temperature operation is desirable to minimize CO poisoning at the anode and to enhance fuel electro-oxidation kinetics. The proton conducting electrolyte, CsH_2PO_4 , meets exactly these requirements, and the authors have successfully demonstrated elsewhere hydrogen/oxygen fuel cells based on this electrolyte with good long-term stability at operational temperatures of $\sim 250^\circ\text{C}$.² The present work was undertaken with the aim of developing high power-density CsH_2PO_4 -based fuel cells operating on methanol. A key innovation involves the incorporation of a steam reforming catalyst for the conversion of methanol to hydrogen (and CO_2) directly in the fuel cell anode chamber.

Experimental

The overall fuel-cell/reformer structure employed is shown in Fig. 1. The fuel cell portion, the fabrication of which is detailed elsewhere,³ consisted of a thin layer of CsH_2PO_4 (26-77 μm thick) sandwiched between two electrocatalyst layers comprised of a mixture of CsH_2PO_4 , carbon black, electrocatalyst particles, and a fugitive pore-former. This component was, in turn, sandwiched between two porous stainless steel supports which served as gas diffusion electrodes. The electrocatalyst in the cathode was Pt (7.7 mg/cm^2), 50 mass % in the form of Pt black and the remainder supported on carbon. As the anode electrocatalyst Pt-Ru was employed (5.6 mg/cm^2 Pt and 2.9 mg/cm^2 Ru), formed of a mixture of $\text{Pt}_{0.5}\text{Ru}_{0.5}$ black (comprising 85 mass % of the metals in the anode) and Pt-Ru (2:1 mass ratio) supported on carbon. The active areas of the cathode and anode were 2.3-2.9 cm^2 and 1.74 cm^2 , respectively. The total measured current and power were divided by the area of the anode to obtain current and power densities.

The reformer was Cu-ZnO supported on Al_2O_3 , a well known

catalyst system for methanol reforming.⁴ A composite comprised of CuO, 30 wt % ZnO 20 wt % Al_2O_3 (CuO, 31 mol % ZnO, 16 mol % Al_2O_3) was prepared by co-precipitation from aqueous solution.^{5,6} Copper, zinc, and aluminum nitrate were dissolved in water (total metal concentration of 1 mol/L) and added to an aqueous solution of sodium carbonate (1.1 mol/L). The resulting precipitate was rinsed with deionized water, filtered, and dried in air at 120°C for 12 h. The dried powder (1 g) was lightly pressed into the form of a disk, 3.1 mm thick and 15.6 mm in diameter, then calcined at 350°C for 2 h. This disk was placed adjacent to the anode-side gas diffusion electrode (see Fig. 1). The copper oxide was reduced to metallic copper by exposure to hydrogen for 2 h in the fuel cell test station prior to fuel cell measurements.

Fuel cells were operated both with and without the reformer, and, in addition to methanol, using hydrogen, reformat (a mixture of H_2 , CO, and CO_2 in a 74.7:0.985:24.3 volume ratio), and ethanol as the fuel (see Table I). In the case of hydrogen, the fuel was supplied at a rate of 100 standard cm^3/min and was humidified to a water partial pressure of 0.3 atm by passing through hot water (70°C). Methanol and ethanol fuels were premixed with water (to dilution levels of 43 and 36 vol %, respectively) and delivered to the fuel cell using a vaporizer. In addition, commercial vodka (Absolut, Sweden) with a nominal ethanol concentration of 40 vol % was also employed. To permit direct comparisons, the hydrogen, alcohol, and reformat fuels were supplied to the anode at equivalent hydrogen flow rates,

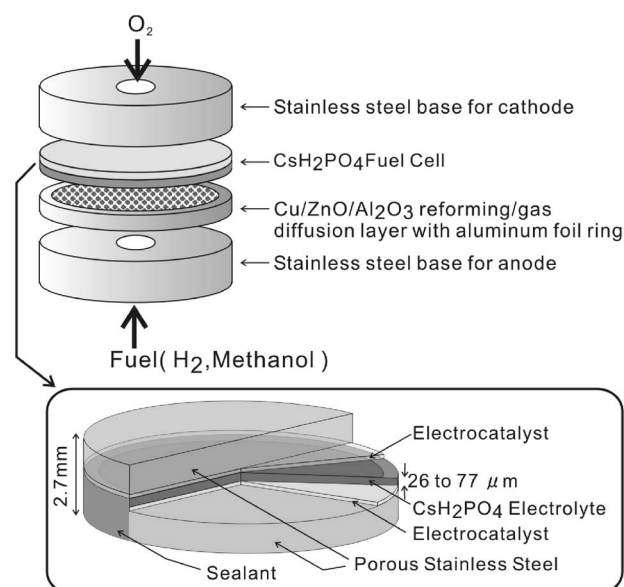


Figure 1. Schematic diagram of an internal-reforming solid acid fuel cell.

^a Present address: Materials Science and Engineering, Kyoto University, Sakyo, Kyoto 606-8501 Japan.

^b Present address: Superprotonic, Inc., Pasadena, CA 91101, USA

^z E-mail: smhaile@caltech.edu

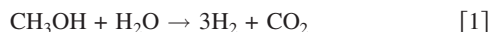
assuming complete reforming. At the cathode, the gas was supplied at a rate of 100 standard cm^3/min and also humidified to 0.3 atm, again, by passing the gas through hot water. Cells were operated at 240-260°C. The theoretical (or Nernstian) open-circuit voltage (OCV) under these conditions is 1.15 V, again, assuming complete reforming for the alcohol fuels.

Results and Discussion

Typical polarization curves obtained from the two different types of cells, one configured with a reformer and one without are presented in Fig. 2. The effectiveness of the reformer in enhancing fuel cell power output is immediately evident. The fuel cell configured with a reformer delivered a peak power output from methanol almost as high as it did from neat hydrogen, 226 vs 270 mW/cm^2 (Fig. 2A). Furthermore, the OCVs for these two fuels were almost identical (962 and 976 mV for the hydrogen and methanol, respectively). These values are somewhat lower than the theoretical OCV because of the difficulties in obtaining reliable seals at such high temperatures using polymer sealants. Elsewhere it has been demonstrated that theoretical OCVs can be obtained from solid acids if the sealant is exposed to less severe conditions.⁷

In the absence of the reformer, the power output from methanol dropped to less than half that obtained from hydrogen, 148 vs 335 mW/cm^2 at peak power, and the OCV dropped by almost 100 mV from 983 to 879 mV (Fig. 2B). Comparing the power outputs of the two cells when operated on neat hydrogen, the slightly lower power from the cell incorporating the reformer is simply a result of the somewhat thicker membrane. Specifically, the data in Fig. 2A were obtained from a fuel cell with a 47 μm thick electrolyte and those of Fig. 2B from a fuel cell with a 34 μm thick electrolyte.

The fuel cell operated with reformat fuel (in the absence of a reformer catalyst layer) exhibited power output almost comparable to that of neat hydrogen (305 mW/cm^2 at peak power vs 335 mW/cm^2). Thus, despite the almost 1% CO in the fuel stream, there is little to no poisoning of the Pt-Ru catalyst. This is presumably a consequence of the relatively high temperature of fuel cell operation. The reformat results further suggest that even modest improvements in the development of a reforming catalyst to more efficiently catalyze the methanol steam reforming reaction



may result in methanol fuel cells with power densities comparable to those obtained from hydrogen fuel cells. This is in stark contrast to PEM fuel cells, in which direct operation on methanol typically results in power outputs that are only about 15% of that from hydrogen.⁸

Because of the tremendous challenges of steam reforming ethanol,⁹ which normally requires temperatures of 350°C or higher even for the best catalysts,¹⁰ power densities obtained from this fuel were lower than from methanol, as shown in Fig. 3. Nevertheless, the peak power densities obtained from ethanol (36 vol % in H_2O) and even commercial vodka were as high as $\sim 100 \text{ mW}/\text{cm}^2$. Furthermore, the OCVs, $\sim 950 \text{ mV}$, were higher than those obtained from methanol fuel cells in the absence of a reformer, again demonstrating that benefit is derived from the integration of the reformer

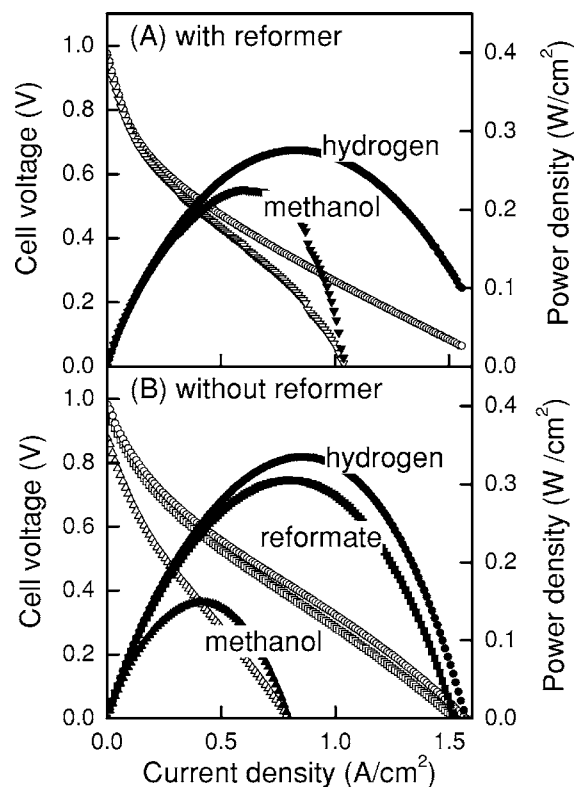


Figure 2. Cell voltage (open symbols) and power density (closed symbols) curves obtained when using pure hydrogen (H_2), premixed reformat (H_2 , 24.3% CO_2 , 0.985% CO), and methanol (H_2O , 43 vol % CH_3OH) fuels with a solid acid fuel cell device comprised of (A) a CsH_2PO_4 -fuel cell (cell 2, Table I) at 260°C with a methanol reformer (Cu-ZnO/ Al_2O_3 catalyst layer) and (B) a CsH_2PO_4 -fuel cell (cell 4, Table I) at 240°C without a reformer.

catalyst layer into the fuel cell anode chamber. Given the presumably high impurity content in the commercial vodka, the results additionally demonstrate the tolerance of the fuel cell anode catalyst to impurities at moderate temperatures.

A more quantitative analysis of the performance of these cells (which have slightly different thicknesses and certainly differences in cathode microstructures) can be achieved by estimating the overpotentials at the anodes, η_{anode} . The anode-overpotential (the drop in voltage across the anode-electrolyte interface) affects the overall cell voltage according to

$$V_{\text{cell}} = V_{\text{ocv}}^{\text{N}} - (\eta_{\text{cathode}} + iR + \eta_{\text{anode}}) \quad [2]$$

where $V_{\text{ocv}}^{\text{N}}$, η , i , and R are, respectively, the Nernstian voltage (expected value at open circuit), the overpotential (at the electrodes), the current density, and the ohmic resistance of the cell. For any given cell, the ohmic drop in voltage as a function of current density (the iR term) is the same (irrespective of the measurement conditions). Moreover, because all measurements were performed with a

Table I. Experimental conditions employed in fuel cell measurements.

Cell	Reformer	Electrolyte thickness, μm	Operational temperature, °C	Fuels
1	Yes	77	260	Methanol (43 vol %), neat hydrogen
2	Yes	47	260	Methanol (43 vol %), neat hydrogen ^b
3	No	26 ^a	240 and 260	Methanol (43 vol %), neat hydrogen, reformat (H_2 , 24.3% CO_2 , 0.985% CO)
4	No	34 ^a	240	Methanol (43 vol %), neat hydrogen, reformat (H_2 , 24.3% CO_2 , 0.985% CO)

^a 2.5 vol % SiO_2 was added to the CsH_2PO_4 electrolyte to provide mechanical support to these thin membranes.

^b This cell also operated using ethanol (36 vol % in H_2O) and vodka (40 vol % ethanol) as the fuel.

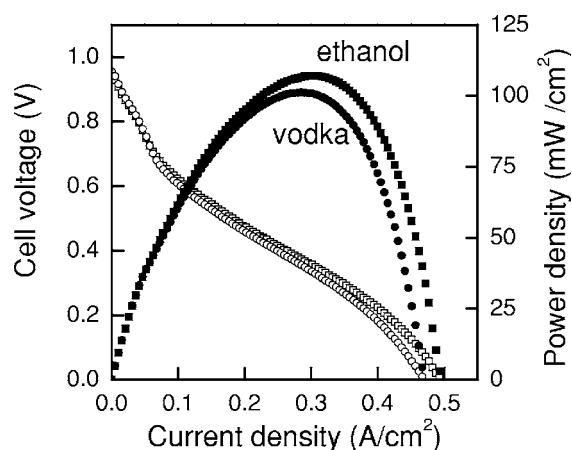


Figure 3. Cell voltage (open symbols) and power density (closed symbols) curves obtained from integrated reformer and SAFC power generators (SAFC = solid acid fuel cell) using ethanol (36 vol % in H₂O) and vodka (40 vol % ethanol) as the fuel. See Table I for details of fuel cell characteristics.

fixed oxygen flow rate, the cathodic overpotentials for any given cell are also identical regardless of the fuel employed. Thus, for any given cell, if we subtract the cell polarization measured under hydrogen/oxygen conditions, $V_{\text{cell}}^{\text{H}_2}$, from the total polarization, $V_{\text{cell}}^{\text{fuel}}$, we obtain a measure of the anode behavior relative to its behavior under neat hydrogen

$$V_{\text{cell}}^{\text{fuel}} - V_{\text{cell}}^{\text{H}_2} \cong \eta_{\text{anode}}^{\text{fuel}} - \eta_{\text{anode}}^{\text{H}_2} \quad [3]$$

The difference term of Eq. 3 is plotted as a function of current density in Fig. 4 for methanol fuel cells both with and without a reformer, and for reformat fuel cells (in which a reformer was not employed). The strong similarity between the behavior of reformat and hydrogen in these fuel cells, which reflects the excellent CO tolerance, is particularly evident from this representation of the data, as is the reproducibility of the anode behavior. There is only a small linear dependence of anode overpotential on current density. It is likely that this voltage drop is due simply to gas dilution effects.

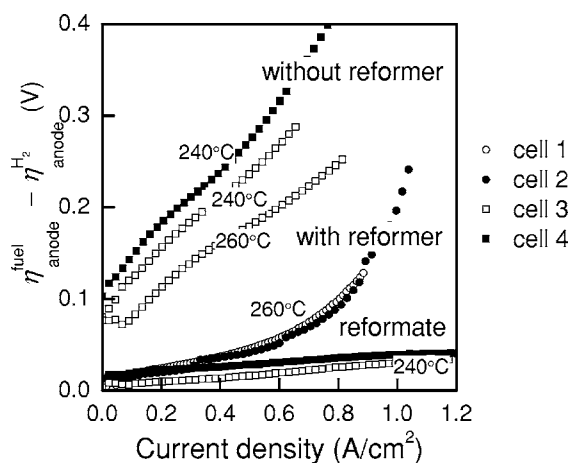


Figure 4. Difference of anode overpotential ($\eta_{\text{anode}}^{\text{fuel}} - \eta_{\text{anode}}^{\text{H}_2}$) as a function of current density between supplying hydrogen (H₂) and methanol or reformat fuel using a solid acid fuel cell (Table I, cells 1-4). Data obtained are for methanol fuel in the absence of a reformer (Table I, cells 3 and 4), methanol fuel in the presence of a reformer (Cu-ZnO/Al₂O₃ catalyst layer) (Table I, cells 1 and 2), and premixed reformat fuel (H₂, 24.3% CO₂, 0.985% CO) in the absence of a reformer (Table I, cells 3 and 4).

Figure 4 also clearly shows that the performance of the methanol fuel cell incorporating the reformer is comparable to that of the reformat operated fuel cell at low current densities (less than 400 mA/cm²). This suggests that the reformer converts methanol to hydrogen and CO₂ at a rate that is comparable to the rate of electrochemical hydrogen consumption in the fuel cell. At higher current densities, the overpotential increases sharply. We attribute this to kinetic limitations of the reforming reaction. That is, for current densities of 400 mA/cm² and greater, the rate of conversion of methanol over the reforming catalyst is not fast enough to keep pace with the rate at which hydrogen is consumed at the fuel cell anode. In contrast, in the absence of the reformer, the overpotentials for the methanol fuel cells are high at all current densities, ranging from ~0.1 V under open circuit conditions to 0.2-0.3 V at 600 mA/cm². Thus, even at ~250°C, methanol cannot be adequately oxidized and/or reformed on the Pt-Ru anode catalyst so as to yield equilibrium concentrations of protons at the fuel cell anode. In conventional PEM fuel cells, open-circuit voltages are typically even lower than the ~0.88 V obtained here in the absence of a reformer. In those fuel cells, not only is electrocatalysis slow, but there are also losses in voltage due to the methanol permeation across the membrane (methanol cross-over). Furthermore, the methanol concentration used in those cells is low to reduce the permeation rate of methanol (typically ~4 vol % in H₂O) and also contributes to the low OCV.

The power outputs obtained here from alcohol-fueled CsH₂PO₄-fuel cells under ambient pressures is competitive with the highest power densities reported for polymer electrolyte based fuel cells even under high pressure conditions. For example, a peak power density of 335 mW/cm² has been achieved from a direct methanol PEM fuel cell at high temperature (120°C) and pressure (1.8-5.0 atm),¹¹ and this value remains essentially the record in the open literature.⁸ Similarly, a peak power density of 110 mW/cm² has been achieved for a direct ethanol fuel cell operated at 140°C and (4.0-5.5 atm).¹² Note that Bjerrum and co-workers have argued that DMFCs operating at power densities as low as 200 mW/cm² at 0.5 V would be competitive with direct hydrogen fuel cells operating at 500-600 mW/cm² as a consequence of the overall system simplification.¹³ The results reported here meet this goal at ambient pressures, albeit at high Pt and Ru loadings. Efforts are presently underway to reduce the precious metals content of these solid acid fuel cells so as to render them truly competitive, and to improve the flow geometries so as to achieve the high power densities implied by the cells operated on reformat fuel.

While it has not been demonstrated here, a combined SAFC and methanol steam reforming catalyst can, in principle, be configured for tight thermal integration between the exothermic fuel cell reactions and the endothermic reforming reaction. Such a configuration would provide a key advantage for methanol fueled SAFCs over PEM fuel cells operated on externally reformed methanol. This is because in an external reforming system, 59 kJ of heat must be provided to reform one mole of methanol according to Eq. 1. This amount is equivalent to the heat of combustion (effectively, the energy content) of 0.24 moles of hydrogen. Thus, the integrated design presented here is preferable over both direct methanol and reformed methanol systems based on polymer electrolyte membrane fuel cells.

Acknowledgments

This work is funded by the National Science Foundation, Division of Materials Research.

The California Institute of Technology assisted in meeting the publication costs of this article.

References

1. B. Richter and L. D. Schmidt, *Science*, **305**, 340 (2004).
2. D. A. Boysen, T. Uda, C. R. I. Chisholm, and S. M. Haile, *Science*, **303**, 68 (2004).
3. T. Uda and S. M. Haile, *Electrochem. Solid-State Lett.*, **8**, A245 (2005).

4. B. A. Peppley, J. C. Amphlett, L. M. Kearns, and R. F. Mann, *Appl. Catal., A*, **179**, 21 (1999).
5. M. Saito, T. Fujitani, M. Takeguchi, and T. Watanabe, *Appl. Catal., A*, **138**, 311 (1996).
6. Y. Tanaka, T. Utaka, R. Kikuchi, K. Sasaki, and K. Eguchi, *Appl. Catal., A*, **238**, 11 (1993).
7. T. Uda, D. A. Boysen, and S. M. Haile, *Solid State Ionics*, **176**, 127 (2005).
8. R. Dillon, S. Srinivasan, A. S. Arico, and V. Antonucci, *J. Power Sources*, **127**, 112 (2004).
9. G. A. Deluga, J. R. Salge, L. D. Schmidt, and X. E. Verykios, *Science*, **303**, 993 (2004).
10. J. Llorca, N. Homs, J. Sales, and P. R. de la Piscina, *J. Catal.*, **209**, 306 (2002).
11. X. M. Ren, M. S. Wilson, and S. Gottesfeld, *J. Electrochem. Soc.*, **143**, L12 (1996).
12. C. Lamy, A. Lima, V. LeRhun, F. Deline, C. Coutanceau, and J. Leger, *J. Power Sources*, **105**, 283 (2002).
13. Q. Li, R. He, J. O. Jensen, and N. J. Bjerrum, *Chem. Mater.*, **15**, 4896 (2003).